

11. C. Beeri and P. A. Bernstein, "Computational problems related to the design of normal form relational schemas," ACM TODS, 4, No. 1, 30-59 (1979).
12. J. Demetrovics, Ho Thuan, Nguyen Xuan Huy, and Le Van Bao, "Translation of relation schemas, balanced relation schemas and the problem of key representation," J. Inform. Proc. Cybern., EIK-23, No. 2/3, 81-97 (1987).
13. D. Maier, A. O. Mendelson, and Y. Sagiv, "Testing implications of data dependencies," ACM TODS, 4, No. 4, 455-469 (1979).
14. D. Maier, The Theory of Relational Databases, Comput. Sci. Press, Rockville, MD (1983).
15. D. Maier, Y. Sagiv, and M. Yannakakis, "On the complexity of testing implications of functional and join dependencies," J. ACM, 28, No. 4, 680-695 (1981).
16. D. Maier, "Minimum covers in the relational database model," J. ACM, 27, No. 4, 664-674 (1980).
17. J. Demetrovics, Ho Thuan, Nguyen Xuan Huy, and Le Van Bao, "Balanced relation scheme and the problem of key representation," MTA SZTAKI, Közlemények, No. 32, 51-80 (1985).

MODELING OF PLASMA ETCHING IN MICROELECTRONICS

V. P. Derkach, I. P. Bagrii,
and G. A. Chechko

UDC 621.3

Computer simulation and experimental results are used to establish the possibility of efficient control of plasma etching rate and nonuniformities.

Plasma etching is a basic technology for the manufacturing of integrated circuit topologies. The available models [1-6] do not fully reflect the macrokinetics of the plasma etching process and are not suitable for modern equipment. The problem of correct modeling of the etching process therefore remains highly relevant and important in many applications.

The following processes take place in a plasma-chemical reactor: production and recombination of chemically active particles (CAPs) in the volume, convective and diffusive transport of CAPs, chemical reactions between CAPs and the etched material, heterogeneous recombination of CAPs. In a general form, the plasma etching process can be described by a system of differential equations

$$\rho \frac{d\vec{v}}{dt} = -\text{grad } p + \mu \Delta \vec{v} + \vec{f}, \quad (1)$$

$$\text{div } \vec{v} = 0, \quad (2)$$

$$\frac{\partial c_i}{\partial t} + (\vec{v} \text{ grad } c_i) = D_i \Delta c_i \pm Q_{0i}, \quad (3)$$

where ρ is the gas density, \vec{v} is the flow velocity vector, p is the pressure, μ is the viscosity of the gas, \vec{f} is the volume force, c_i is the concentration of CAPs of species i , D_i is the diffusion coefficient of CAPs of species i , Q_{0i} is the capacity of the volume source responsible for production or recombination of CAPs of species i .

Translated from Kibernetika, No. 5, pp. 27-33, September-October, 1990. Original article submitted December 21, 1988.

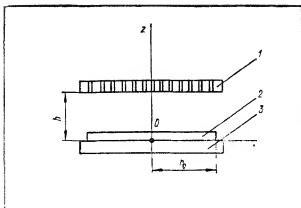


Fig. 1. Schematic diagram of the individual treatment reactor: 1) perforated anode, 2) plate, 3) cathode.

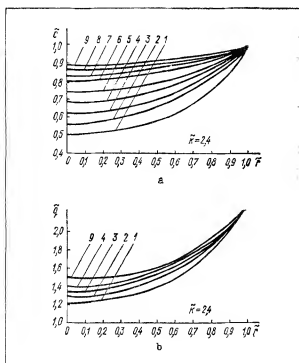


Fig. 2. Distribution of CAP concentration (a) and etching rate (b) over the plate radius for $\tilde{k} = 2.4$ and various h_0 : 1) $h_0 = 0.1$, 2) $h_0 = 0.2$, 3) $h_0 = 0.3$, 4) $h_0 = 0.4$, 5) $h_0 = 0.5$, 6) $h_0 = 0.6$, 7) $h_0 = 0.7$, 8) $h_0 = 0.8$, 9) $h_0 = 0.9$.

The Navier-Stokes equation (1) describes the hydrodynamic motion of the gas in the reactor. The continuity equation (2) is an expression of the law of conservation of matter. Equation (3) describes convective diffusion during plasma etching. Note that the parameter Q_{0i} describes only volume processes. Particles produced or destroyed on the

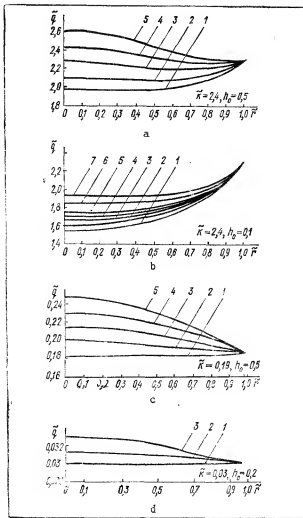


Fig. 3. Distribution of etching rate over the plate radius for various \bar{k} and h_0 [a] $\bar{k} = 2.4$, $h_0 = 0.5$, b) $\bar{k} = 2.4$, $h_0 = 0.1$, c) $\bar{k} = 0.19$, $h_0 = 0.5$, d) $\bar{k} = 0.03$, $h_0 = 0.2$] and various values of the parameter A: 1) $A = 0$, 2) $A = 0.1$, 3) $A = 0.2$, 4) $A = 0.3$, 5) $A = 0.4$, 6) $A = 0.5$, 7) $A = 0.8$.

surface are allowed for by boundary conditions. The boundary conditions for the system of equations (1)-(3) have the following form:

$$\bar{v} = 0 \text{ on all surfaces,} \quad (4)$$

$$Ddc_1/dn = kc_1^m \text{ on all surfaces,} \quad (5)$$

$$c_1 \text{ is finite at the reactor center,} \quad (6)$$

where n is the direction of the normal to the surface, k is the rate constant of the surface reaction (chemical reaction or recombination process), m is the kinetic order of the reaction. In physical terms, expression (5) describing the surface reaction kinetics implies that the flow of CAPs on the surface is determined by surface reactivity.

Solving the system of equations (1)-(6) is a fairly complex undertaking. It can be simplified if we exploit some specific features of the plasma etching process. Calculations show that the Peclet number, which characterizes the efficiency of diffusion and convective processes, is 0.05-0.3 [1]. For comparison, the Peclet number of a liquid is 10^4 .

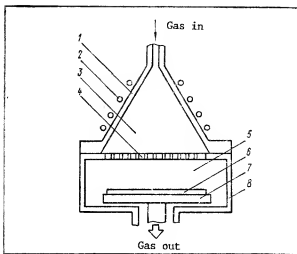


Fig. 4. Schematic diagram of the reactor in the PLAZMA 125I facility: 1) quartz cone, 2) HF inductor, 3) plasma production zone, 4) perforated screen, 5) treatment zone, 6) plate, 7) cathode, 8) body.

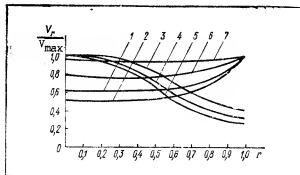


Fig. 5. Etching nonuniformity of polysilicon (1-5), silicon nitride (6), and silicon oxide (7) in the PLAZMA 125I facility in a $\text{SF}_6 + 20\% \text{ O}_2$ mixture at 160 Pa pressure, 40 W HF power, for various perforated anode designs from Table I: 1) anode No. 5, 2) anode No. 4, 3) anode No. 3, 4) anode No. 1, 5) anode No. 2, 6, 7) anode No. 5.

Plasma etching therefore may be regarded as a quasifixed system. Moreover, since the etching time is much greater than the CAP lifetime, plasma etching also may be viewed as a quasistationary system. We also assume that CAP production and recombination is uniform throughout the volume, so that the system of equations (1)-(6) reduces to

$$D_i \Delta c_i - k_p c_i^l + G_i = 0 \quad (7)$$

with the boundary conditions

$$\frac{D_i \Delta c_i}{dn} = k_i c_i^m \text{ on all surfaces,} \quad (8)$$

$$c_i \text{ is finite at the reactor center,} \quad (9)$$

TABLE I

| Anode | Zone | Zone radius, mm | Grid spacing, mm | Hole diameter, mm | Anode transparency, rel. units |
|-------|------|-----------------|------------------|-------------------|--------------------------------|
| 1 | 1 | 60 | 4×4 | 2,5 | 0,3 |
| 2 | 1 | 40 | 4×4 | 2,5 | 0,3 |
| | 2 | 60 | 4×4 | 5 | 1 |
| 3 | 1 | 25 | 4×4 | 2,5 | 0,3 |
| | 2 | 40 | 5×5 | 2,5 | 0,16 |
| | 3 | 60 | 6×6 | 2,5 | 0,1 |
| 4 | 1 | 40 | — | — | 0 |
| | 2 | 60 | 4×4 | 2,5 | 0,3 |
| 5 | 1 | 25 | 8×8 | 2,5 | 0,06 |
| | 2 | 40 | 4×4 | 2,5 | 0,3 |
| | 3 | 60 | 4×4 | 5 | 1 |

where $k_{p_i}c_i^\ell$ and G_i are the homogeneous recombination rate and the production rate of CAPs of species i , k_{p_i} is the homogeneous recombination rate constant, ℓ is the kinetic order of the reaction. In general, the coefficients D_i , k_{p_i} , k_i may be variable.

Equation (7) with boundary conditions (8)–(9) is the basic macrokinetic equation of plasma etching. Solving this equation, we obtain the distribution of the CAP concentration, determine the derivative $\partial c_i / \partial n$, and calculate the etching rate $v = \sum_i j_i = \sum_{i=1}^n D_i (\partial c_i / \partial n)$ in flow units [$\text{cm}^{-2}\text{sec}^{-1}$]. In the reactor this equation describes the loading effect,

on the plate it describes the rate, selectivity, and nonuniformity of etching, and on an element of the circuit topology it describes the etching profile.

Let us consider the limits of applicability of the proposed model. The diffusion approximation is valid when the CAP free path λ is much less than the characteristic dimensions of the system. For plasma etching in the pressure range 10–100 Pa, $\lambda \approx 100\text{--}10 \mu\text{m}$. For the reactor and the plate, these conditions are satisfied; for a topology element, $\lambda \sim d$. Equations (7)–(9) therefore must be used with care when describing plasma etching processes on a topology element. If $\lambda \gg d$, then the diffusion approximation is inapplicable to the description of plasma etching on a topology element and we have to consider free-molecular motion of the CAPs.

Solving equations (7)–(9) for a specific plasma-etching reactor by numerical methods, we obtain all the process characteristics, but this is a complicated and time-consuming process. Specializing the plasma-etching conditions and the boundary conditions of the problem, we can apply the general model to obtain a number of interesting practical results. As an example, consider the plasma etching of silicon-containing materials (Si^* , Si_3N_4 , SiO_2) in an individual treatment installation with $\text{SF}_6 + \text{O}_2$ plasma.

The recent increase of plate diameters has encouraged the transition to individual treatment facilities. In some facilities, the plasma discharge zone is separated by a metallic grid from the processing zone. The schematic form of the plasma reactor in such systems is shown in Fig. 1. For definiteness, we refer to the lower electrode as the cathode and to the upper electrode as the anode. The etching plate is located on the cathode; the anode is perforated. This anode design makes it possible to investigate etching nonuniformities for various concentration profiles of the CAPs arriving at the plate surface.

Since CAPs are generated only in the plasma discharge zone, etching in $\text{SF}_6 + \text{O}_2$ plasma is performed by CAPs of one species only — fluorine atoms. The chemical etching reactions are first-order reactions in CAP concentration and CAP recombination occurs only on the etching surface [8]. Assuming that the CAP diffusion coefficient is independent of CAP concentration, we obtain from the general equation (7) $\Delta c = 0$.

Initially, let us consider the determination of etching nonuniformity in the absence of CAP sources on the anode surface. The diffusion equation in cylindrical coordinates for the axially symmetric case has the form

$$\frac{\partial^2 c}{\partial r^2} + \frac{1}{r} \frac{\partial c}{\partial r} + \frac{\partial^2 c}{\partial z^2} = 0 \quad (10)$$

with the boundary conditions

$$\begin{aligned} c(r_0, z) &= c_0, \quad D \cdot \frac{\partial c}{\partial z}(r, h) = 0, \\ D \cdot \frac{\partial c}{\partial z}(r, 0) &= k \cdot c(r, 0), \end{aligned} \quad (11)$$

where c_0 is the given concentration at the reactor inlet (it is determined experimentally), h is the interelectrode distance, r_0 is the plate radius.

We introduce a new concentration function $C(r, z) = c - c_0$. Problem (10), (11) is transformed to the form

$$\frac{\partial^2 C}{\partial r^2} + \frac{1}{r} \frac{\partial C}{\partial r} + \frac{\partial^2 C}{\partial z^2} = 0, \quad (12)$$

$$\begin{aligned} C(r_0, z) &= 0, \quad \frac{\partial C}{\partial z}(r, h) = 0, \\ D \frac{\partial C}{\partial z}(r, 0) &= kC(r, 0) + kc_0. \end{aligned} \quad (13)$$

The solution of problem (12), (13) is best sought in dimensionless form:

$$\frac{\partial^2 \tilde{C}}{\partial \tilde{r}^2} + \frac{1}{\tilde{r}} \frac{\partial \tilde{C}}{\partial \tilde{r}} + \frac{\partial^2 \tilde{C}}{\partial \tilde{z}^2} = 0, \quad (14)$$

$$\begin{aligned} \tilde{C}(1, \tilde{z}) &= 0, \quad \frac{\partial \tilde{C}}{\partial \tilde{z}}(\tilde{r}, h_0) = 0, \quad \frac{\partial \tilde{C}}{\partial \tilde{z}}(\tilde{r}, 0) = \\ &= \tilde{k}\tilde{C}(\tilde{r}, 0) + \tilde{k}, \end{aligned} \quad (15)$$

where $\tilde{C} = C/c_0$, $\tilde{r} = r/r_0$, $\tilde{z} = z/r_0$, $\tilde{k} = r_0 k/D$, $h_0 = h/r_0$, $0 \leq \tilde{r} \leq 1$, $0 \leq \tilde{z} \leq h$. The general solution of the problem obtained by separation of variables is representable in series form

$$\tilde{C}(\tilde{r}, \tilde{z}) = \sum_{n=1}^{\infty} [A_n \cdot \text{Sh} \mu_n(h_0 - \tilde{z}) + B_n \cdot \text{Sh} \mu_n \tilde{z} J_0(\mu_n \tilde{r})], \quad (16)$$

where $\lambda_n = \mu_n^2$ and μ_n ($n = 1, 2, \dots, \infty$) are the roots of the equation $J_0(\mu) = 0$. The series coefficients A_n and B_n are given by the expressions

$$A_n = B_n \cdot \text{ch} \mu_n h_0, \quad (17)$$

$$\begin{aligned} B_n &= 2k/\{\mu_n^2 J_1(\mu_n) \cdot [1 - \text{ch} \mu_n h_0 (\text{ch} \mu_n h_0 + \\ &+ \tilde{k} \cdot \text{Sh} \mu_n h_0)]\}, \end{aligned} \quad (18)$$

where $J_0(\mu)$, $J_1(\mu)$ are Bessel functions.

Let us write dimensionless expressions for the CAP concentration at the anode surface for $z = h_0$ and for the flow on the etched plate for $z = 0$, which is equivalent to the etching rate:

$$\tilde{C}(\tilde{r}, h_0) = \sum_{n=1}^{\infty} B_n \text{Sh} \mu_n h_0 \cdot J_0(\mu_n \cdot \tilde{r}) + 1, \quad (19)$$

$$\tilde{q} = \frac{\partial \tilde{C}}{\partial z}(\tilde{r}, 0) = \sum_{n=1}^{\infty} \mu_n (B_n - A_n \cdot \text{Sh} \mu_n h_0). \quad (20)$$

We used formulas (19) and (20) in some computations, which revealed a marked decrease of CAP concentration in the direction of the OZ axis (Fig. 2a). Indeed, as the CAPs progress by diffusion from the edge of the plate to its center, the CAPs are gradually absorbed by the chemical reaction on the etching surface.

It follows from (19) that if a gas mixture is additionally forced through the anode surface, supplying a supplementary concentration distribution density near the anode according to the formula

$$j_g = - \sum_{n=1}^{\infty} B_n \cdot \text{Sh} \mu_n h_0 \cdot J_0(\mu_n \tilde{r}),$$

the CAP concentration for $z = h_0$ will be maintained equal to c_0 . This, however, may be insufficient for ensuring uniform etching with acceptable tolerance over the entire surface of the plate in the full range of parameter variation in practice. Such uniformity apparently can be ensured only if the CAP concentration at the anode surface is distributed by the law

$$\tilde{C}(\tilde{r}, h) = c_0 + g(\tilde{r}),$$

where the function $g(\tilde{r})$ is unknown and, by axial symmetry of the problem, satisfies the conditions $g(0) = 0$ and $g(1) = 0$. Thus, uniform etching can be achieved only if the additional inflow of gas mixture through the perforated anode modifies the plasma discharge so that the following supplementary CAP concentration is established on the anode at $z = h_0$:

$$F_g(\tilde{r}) = g(\tilde{r}) - \sum_{n=1}^{\infty} B_n \cdot \text{Sh} \mu_n h_0 \cdot J_0(\mu_n \tilde{r}).$$

Calculations show that the function $g(\tilde{r})$ must be positive.

In general, the problem of improving the etching uniformity and finding the function $F(\tilde{r})$ can be solved mathematically, by specifying a constant CAP flow at the plate surface for $z = 0$ (constant etching rate over the plate). In dimensionless variables, the problem takes the form

$$\frac{\partial^2 c}{\partial r^2} + \frac{1}{r} \frac{\partial c}{\partial r} + \frac{\partial^2 c}{\partial z^2} = 0, \quad (21)$$

$$c(r_0, z) = c_0, \quad c(r, h) = j(r), \quad D \frac{\partial c}{\partial z}(r, 0) = q = kc_1, \quad (22)$$

where c_1 is a constant.

We solve problem (21), (22) by separation of variables. The solution is represented by the series

$$c(r, z) = c_0 + \sum_{n=1}^{\infty} \left[A_n \cdot \text{Sh} \frac{\mu_n}{r_0} (h - z) + B_n \cdot \text{Sh} \frac{\mu_n}{r_0} z \right] \cdot J_0 \left(\frac{\mu_n}{r_0} r \right), \quad (23)$$

where A_n and B_n are given by the expressions

$$B_n = \frac{2}{r_0^2 \cdot J_1^2(\mu_n) \operatorname{Sh}\left(\frac{\mu_n}{r_0} h\right)} \left[\int_0^{r_0} r \cdot f(r) \times \right. \\ \left. \times J_0\left(\frac{\mu_n}{r_0} r\right) dr - c_0 r_0^2 J_1(\mu_n)/\mu_n \right],$$

$$A_n = \frac{4}{r_0^2 J_1^2(\mu_n) \operatorname{Sh}^2\left(\frac{\mu_n}{r_0} h\right)} \left[\int_0^{r_0} r f(r) J_0 \times \right. \\ \left. \times \left(\frac{\mu_n}{r_0} r\right) dr - c_0 r_0^2 J_1(\mu_n)/\mu_n \right] - \frac{2 k c_1 r_0}{D \mu_n^2 \cdot J_1(\mu_n) \cdot \operatorname{Ch}\frac{\mu_n}{r_0} h}$$

We need an additional condition in order to find the unknown function $f(r)$. Isolate a cylinder with cross-section radius r_0 within the active part of the reactor and define the CAP flow through all the surfaces of this cylinder: Q_1 is the CAP flow through the cylinder wall, Q_2 is the CAP flow through the perforated anode surface, and Q_3 is the CAP flow to the etching plate. By the law of mass conservation, we clearly have $Q_1 + Q_2 = Q_3$ and after simple manipulations we obtain in expanded form

$$\sum_{n=1}^{\infty} \left(B_n - A_n \cdot \operatorname{Ch}\frac{\mu_n h}{r_0} \right) \cdot J_1(\mu_n) = \frac{k r_0 c_1}{2D}. \quad (24)$$

For a given flow $q = kc_1$, the unknown function $f(r)$ can be found numerically from the integral equation (24). When the flow q , and therefore the etching rate, are variable, the function $f(r)$ will also vary. Numerical solution of Eq. (24) involves considerable difficulties and requires a special mathematical apparatus, because the problem is ill-posed. This means that there may exist several functions $f(r)$, all of which satisfy Eq. (24), and the function $f(r)$ determined by the numerical method is not necessarily the unique solution that corresponds to the physical content of the problem.

The problem of improving the etching uniformity is thus better solved by an approximate fitting of the function $f(r)$. From physical considerations we conclude that it has a nearly parabolic form: $f(r) = c_0 + A(r_0^2 - r^2) = c_0 + g(r)$, where A is an unknown constant. Varying A , we can obviously ensure approximate constancy of the flow (etching rate) on the plate surface.

The diffusion equation and the boundary conditions in this case have the form

$$\frac{\partial^2 c}{\partial r^2} + \frac{1}{r} \frac{\partial c}{\partial r} + \frac{\partial^2 c}{\partial z^2} = 0, \quad (25)$$

$$c(r_0, z) = c_0, \quad c(r, h) = c_0 + A(r_0^2 - r^2), \quad (26)$$

$$D \frac{\partial c}{\partial z}(r, 0) = kc(r, 0).$$

Introducing a new concentration function $C(r, z) = c(r, z) - c_0$ and changing to dimensionless variables, we transform problem (25), (26) to

$$\frac{\partial^2 \bar{C}}{\partial \bar{r}^2} + \frac{1}{\bar{r}} \frac{\partial \bar{C}}{\partial \bar{r}} + \frac{\partial^2 \bar{C}}{\partial \bar{z}^2} = 0, \quad (27)$$

$$\bar{C}(1, \bar{z}) = 0, \quad \bar{C}(\bar{r}, h_0) = \tilde{A}(1 - \bar{r}^2),$$

$$\frac{\partial C}{\partial z}(\tilde{r}, 0) = \tilde{k}\tilde{C}(\tilde{r}, 0) + \tilde{k}, \quad (28)$$

where $\tilde{A} = Ar_0^2/c_0$, $\tilde{z} \in [0, h_0]$, $\tilde{r} \in [0, 1]$, $k > 0$.

Problem (27), (28) is solved by separation of variables and its solution is represented by series (16) with the coefficients A_n and B_n given by the expressions

$$A_n = (\text{Ch } \mu_n h_0 + \tilde{k} \text{Sh } \mu_n h_0)^{-1} \cdot \{B_n - 2\tilde{k}/[\mu_n^2 \cdot J_1(\mu_n)]\},$$

$$B_n = \{2\tilde{A}/[\mu_n \cdot J_1(\mu_n) \text{Sh } \mu_n h_0]\} \times$$

$$\times \left\{ 1 - [\mu_n/J_1(\mu_n)] \cdot \int_0^1 \tilde{r}^2 J_0(\mu_n \tilde{r}) d\tilde{r} \right\}.$$

Calculation results regarding etching nonuniformity for various parameters h_0 , \tilde{A} , and \tilde{k} are presented in Fig. 3. Analysis of the curves indicates that etching nonuniformity can be altered by forcing an additional gas mixture into the interelectrode space and a CAP distribution density can be chosen for which uniform etching is achieved on the entire plate surface with practically acceptable tolerances. The graphs in Fig. 3 show that as the interelectrode distance increases, the supplementary CAP flow rate forced through the perforated anode must be increased for plasma-etching control. Calculations show that as the coefficient \tilde{k} decreases, the etching uniformity improves, which also facilitates the process of control.

Theoretical modeling of etching rate and nonuniformity leads to a number of important practical conclusions. First, a uniform distribution of CAP concentration on the anode for etching of high- k materials does not ensure uniform etching. Second, by shaping the CAP flow on the etching surface, e.g., by means of a perforated screen, we can control the etching uniformity between wide limits.

Experimental tests of the theoretical results were made on a PLAZMA 12SI individual treatment facility. Films of polysilicon (0.55 μm thick), silicon nitride (0.15 μm), and silicon oxide (0.1 μm) on silicon plates 100 mm in diameter were etched in a $\text{SF}_6 + 20\% \text{O}_2$ mixture at pressures of 160 Pa and 40 W high-frequency power. The reactor is shown schematically in Fig. 4. The plate treatment zone is separated from the plasma production zone by a perforated metallic screen which, on the one hand, protects the plate from bombardment by plasma ions and, on the other, shapes the CAP flow hitting the surface of the plate. The chamber design is very close to the theoretical reactor shown in Fig. 1 and is ideally suited for studies of nonuniform etching under individual treatment conditions: cathode diameter 120 mm, reactor height $h_0 = 30$ mm, plate diameter 100 mm ($r_0 = 50$ mm).

Chamber design and etching technology are developed so as to ensure a uniform concentration of CAPs on the screen surface, and the screen (the anode in our notation) is usually perforated uniformly with constant transparency along the radius. In practice, however, this chamber design does not produce a uniform distribution of CAP concentration in the treatment zone. The solutions obtained above may be used to produce both uniform and nonuniform CAP concentrations. By varying the anode transparency according to a certain law, we can produce the desired CAP distribution profile and with it the desired etching uniformity.

The following method was used to obtain varying anode transparency. The anode radius was partitioned into three zones. Each zone was characterized by a certain grid spacing and hole diameter. By varying the zone radius, the grid spacing in the zone, and the hole diameter, we could regulate the magnitude and the distribution of anode transparency between wide limits. The anode characteristics used in our experiments are listed in Table 1.

Comparison of the theoretical model with experimental results should allow for the fact that the calculations were carried out for certain values of the dimensionless variable \tilde{k} , which is a function both of the discharge and of the interaction of the material with the CAP — the rate constant k of the chemical reaction. The exact value of the rate constant was not available in most cases, although it is well known that $k_{\text{Si}} > k_{\text{Si}_3\text{N}_4} > k_{\text{Si}_2\text{O}_5}$ [9]. Therefore, only a qualitative comparison of the theoretical and experimental values was possible. Polysilicon films have a high rate constant for the reaction with fluorine atoms, the main CAP in the $\text{SF}_6 + \text{O}_2$ discharge. The experiments with these films therefore produced the most significant results.

Etching of polysilicon films with a standard anode of uniform transparency (1 in Table 1) produces a higher etching rate at the center of the plate than at the periphery (Fig. 5, curve 4). This etching pattern is determined by nonuniformity of the initial CAP flow reaching the anode surface in the chamber of our design (Fig. 4). The observed etching pattern could not be changed by varying the technological conditions (pressure, mixture composition, HF power). Application of a perforated anode with the same distribution of transparency (3 in Table 1) enhances the etching nonuniformity. Anodes in which the distribution of transparency is the inverse of the CAP distribution produced by the chamber design (2, 4, 5 in Table 1) alter the etching pattern all the way to complete inversion: the etching rate at the periphery of the plate is higher than at the center (Fig. 5). Similar results, although less sharply pronounced, were also obtained for silicon nitride and silicon oxide etching (Fig. 5).

Experiments have shown, however, that the use of perforated anodes in systems of this kind is in itself insufficient to ensure etching uniformity of polysilicon films which meets modern technological requirements. The existing reactor design does not produce a sufficiently uniform CAP flow along the chamber diameter. It is also necessary to ensure a uniform CAP flow on the anode surface by altering the reactor design.

Note that the numerical values of the plasma etching kinetic constants (CAP diffusion coefficients, etching rate constants, heterogeneous and homogeneous recombination rate constants, CAP production rates) and their dependence on technological process parameters have been little studied [6]. As a result, our model ignores these factors and, while correctly estimating the qualitative picture, it does not pretend to produce an exact description of the process. Further development of the model must account for a number of additional factors, such as the effect of plasma discharge on CAP concentration and transport during etching, ambipolar diffusion of high-energy particles, convective transport of CAPs and high-energy particles, electron and ion bombardment, UV radiation.

Plasma etching, being a heterogeneous chemical reaction which includes CAP production, recombination, transport processes, and chemical reactions on the surface, may be described to first approximation by the CAP diffusion equation of the form $D_l \Delta C_l - k_{p_l} C_l^{\ell} + G_l = 0$ with the boundary conditions of the form $D_l \text{grad } C_l = k_l C_l^m$ reflecting the kinetics of surface reaction. The proposed model describes heterogeneous chemical reactions (on the assumption that the kinetic constants k_l , k_{p_l} , G_l , D_l , ℓ , m , and other factors dependent on external plasma discharge parameters are known) and reflects the macrokinetic features of the plasma etching process. The kinetic constants entering the model may be obtained from experimental data or from special theoretical studies. In application to individual treatment of plates, the model parameters are the geometrical dimensions of the reactor and the plate, the rate constant of the chemical reaction of the CAPs with the material, and plasma discharge parameters (diffusion coefficient and concentration of CAPs).

Our modeling has shown that in order to ensure uniform etching of materials with high chemical rate constants, a nonuniform CAP flow must be produced on the etching surface. A suitable concentration pattern can be created by a perforated anode of variable transparency. The modeling results are supported by experimental etching data for polysilicon, silicon oxide, and silicon nitride in the PLAZMA 125I individual treatment facility with $\text{SF}_6 + 20\% \text{ O}_2$ mixture at 160 Pa pressure and 40 W high-frequency power.

LITERATURE CITED

1. R. C. Alkire and D. J. Economos, "Transient behavior during film removal in diffusion-controlled plasma etching," *J. Electrochem. Soc.*, **132**, No. 3, 648-656 (1985).
2. J. F. Battey, "The effect of geometry on diffusion-controlled chemical reaction rates in plasma," *J. Electrochem. Soc.*, **124**, No. 3, 437-442 (1977).
3. M. Doken and I. Mayata, "Etching uniformities of silicon in $\text{CF}_4 + 4\% \text{ O}_2$ plasma," *J. Electrochem. Soc.*, **126**, No. 12, 2235-2239 (1979).
4. C. J. Mogab, "The loading effect in plasma etching," *J. Electrochem. Soc.*, **124**, No. 8, 1262-1268 (1977).
5. M. J. Kushner, "A kinetic study of the plasma etching process. I. A model for etching of Si and SiO_2 in $\text{C}_n\text{F}_m/\text{H}_2$ and $\text{C}_n\text{F}_m/\text{O}_2$ plasmas," *J. Appl. Phys.*, **53**, No. 4, 2923-2938 (1982).
6. S. N. Ryabov, S. A. Kutolin, and N. I. Baikin, "Physicochemical features of plasma etching processes," in: *Reviews in Electronic Engineering, Ser. 7, Technology, Organization of Production, and Equipment* [in Russian], No. 20 (1981).
7. D. A. Frank-Kamenetskii, *Diffusion and Heat Transfer in Chemical Kinetics* [in Russian], Nauka, Moscow (1967).

8. N. N. Nevzorov, D. I. Slovenskii, and A. F. Shelykhmanov, "Distribution of concentration of chemically active particles in a HF diode reactor at the interface of two materials," Abstracts of papers, 2nd All-Union Seminar on Microtechnology, IPTM Akad. Nauk SSSR, Chernogolovka (1988), p. 88.
9. A. S. Dzyan, L. Yu. Gal'chinskii, I. P. Bagrii, and others, Studies of Plasma Etching Uniformities of Silicon-Containing Materials [in Russian], IK Akad. Nauk UkrSSR, Kiev (1987), pp. 24-31.

METHODS TO FIND THE MOST PREFERRED ELEMENT ON A SET OF PARETO-OPTIMAL DECISIONS

M. V. Mikhalevich

UDC 519.8

Stochastic interactive procedures are considered, based on paired comparison of efficient solutions with parametrization of the Pareto-optimal set. The convergence conditions of these procedures are analyzed.

Multicriterion problems often arise in connection with mathematical modeling of economic, technical, social, and other complex system. Let us consider one of such problems.

Assume that the set D of all feasible solutions is given in E^n . Each (not necessarily feasible) solution x is an m -dimensional vector of criterion values $f(x) = (f_1(x), \dots, f_m(x))$, $m \geq 2$, which is improved by increasing any of the criteria, while keeping the other criteria fixed. It is required to find a solution $x^* \in D$ which corresponds to optimal (in a sense to be defined later) criterion values. This problem will be written in the form

$$(f_1(x), \dots, f_m(x)) \rightarrow \max_{x \in D} \quad (1)$$

Given problem (1), a solution \tilde{x} which for some $y \in D$ satisfies $f_i(\tilde{x}) \leq f_i(y)$ and $f_k(\tilde{x}) < f_k(y)$ for at least one $1 \leq k \leq m$ is a priori not the optimal solution x^* . Eliminating all the solutions \tilde{x} from the feasible set D , we obtain the set \hat{D} of Pareto-optimal (efficient) solutions. If D is closed and bounded and the functions $f_i(x)$ are continuous, then the set \hat{D} is clearly nonempty and at least one of the solutions of the problem $\max_{x \in D} f_i(x)$ belongs to this set.

In various applications, the set \hat{D} usually consists of more than a single solution [1]. In some problems of the form (1) we have [2] $\hat{D} = D$, and additional assumptions are needed in order to determine x^* . In what follows we assume that a decision maker exists who is capable of comparing any two solutions (in particular, any two solutions from \hat{D}) by the corresponding criterion values and choosing that which is better. The search of the solution x^* of problem (1) is an interactive procedure by which the decision maker chooses the best solution from \hat{D} . The decision maker compares the criterion vectors generated by computer; the function of the computer in this case is to make sure that these vectors represent feasible (and, moreover, efficient) solutions.

The mathematical model of the decision maker in this interactive procedure is a binary relation R defined on the set of all m -dimensional vectors f as follows: $f^{(1)}Rf^{(2)}$ if the decision maker judges the solution with the criterion value vector $f^{(1)}$ not worse than the solution with the criterion vector $f^{(2)}$. Problem (1) now can be restated as the problem of finding a solution $x^* \in D$ which for any $x \in D$ satisfies $f(x^*)Rf(x)$. The purpose of this paper is to describe methods for solving this problem under appropriate assumptions about the properties of D and R .

Let D be a convex compactum in E^n and let the relation R be complete, reflexive, transitive, and continuous [3]. The distinctive feature of the methods considered in this paper is that all the solutions presented to the decision maker